OXFORD

SOT | Society of Toxicology
academic.oup.com/toxsci

TOXICOLOGICAL SCIENCES, 184(2), 2021, 236–251

doi: 10.1093/toxsci/kfab114
Advance Access Publication Date: 21 September 2021
Research Article

Neuroligin-1 Is a Mediator of Methylmercury Neuromuscular Toxicity

Jakob T. Gunderson, Ashley E. Peppriell, Ian N. Krout, Daria Vorojeikina, and Matthew D. Rand[1]

Department of Environmental Medicine, University of Rochester School of Medicine and Dentistry, Rochester, New York 14642, USA

[1]To whom correspondence should be addressed. E-mail: Matthew_Rand@urmc.rochester.edu.

ABSTRACT

Methylmercury (MeHg) is a developmental toxicant capable of eliciting neurocognitive and neuromuscular deficits in children with *in utero* exposure. Previous research in *Drosophila melanogaster* uncovered that developmental MeHg exposure simultaneously targets the developing musculature and innervating motor neuron in the embryo, along with identifying *Drosophila neuroligin 1* (*nlg1*) as a gene associated with developmental MeHg sensitivity. Nlg1 and its transsynaptic partner neurexin 1 (Nrx1) are critical for axonal arborization and NMJ maturation. We investigated the effects of MeHg exposure on indirect flight muscle (IFM) morphogenesis, innervation, and function via flight assays and monitored the expression of NMJ-associated genes to characterize the role of Nlg1 mediating the neuromuscular toxicity of MeHg. Developmental MeHg exposure reduced the innervation of the IFMs, which corresponded with reduced flight ability. In addition, *nlg1* expression was selectively reduced during early metamorphosis, whereas a subsequent increase was observed in other NMJ-associated genes, including *nrx1*, in late metamorphosis. Developmental MeHg exposure also resulted in persistent reduced expression of most *nlg and nrx* genes during the first 11 days of adulthood. Transgenic modulation of *nlg1 and nrx1* revealed that developing muscle is particularly sensitive to *nlg1* levels, especially during the 20–36-h window of metamorphosis with reduced *nlg1* expression resulting in adult flight deficits. Muscle-specific overexpression of *nlg1* partially rescued MeHg-induced deficits in eclosion and flight. We identified Nlg1 as a muscle-specific, NMJ structural component that can mediate MeHg neuromuscular toxicity resulting from early life exposure.

Key words: methylmercury; *Drosophila melanogaster*; neuromuscular junction; neuroligin-1.

Methylmercury (MeHg) is a ubiquitous, environmental pollutant that accumulates in seafood and, at sufficient doses, harms human health (Chen *et al.*, 2008; Cunningham *et al.*, 2003; Hong *et al.*, 2012). Historical accidental poisonings in Japan and Iraq identified the developing fetus as a highly sensitive target of MeHg (Bakir *et al.*, 1973; Harada, 1995). Prenatal MeHg exposure can cause cognitive and motor deficits in children, including lower IQ, reductions in visuospatial perception, ataxia, muscle weakness, decreased muscle tone, and perturbed movements and reflexes (Antunes Dos Santos *et al.*, 2016; Bakir *et al.*, 1973; Harada, 1995; McKeown-Eyssen *et al.*, 1983). The clinical neuromotor outcomes described in children with *in utero* MeHg exposure are consistent with identified neuro- and myotoxic mechanisms of MeHg, including reduced neuroblast proliferation (Burke *et al.*, 2006; Rodier *et al.*, 1984), inhibited neuroblast and myoblast differentiation (Sager *et al.*, 1984; Culbreth and Rand, 2020; Prince and Rand, 2018), diminished axonal or neurite outgrowth (Fujimura and Usuki, 2015; Fujimura *et al.*, 2016; Rand *et al.*, 2009), altered neuronal and myogenic gene expression (Culbreth and Rand, 2020; Fujimura *et al.*, 2009, 2012; Gonzalez *et al.*, 2005; Peppriell *et al.*, 2020; Prince and Rand, 2017), perturbed myomorphology (Gunderson *et al.*, 2020; Montgomery *et al.*, 2014;

Peppriell *et al.*, 2020; Usuki *et al.*, 1998), and reduced neurotransmission (Atchison and Narahashi, 1982; Candura *et al.*, 1997; Carratu *et al.*, 2006). Despite the wealth of literature covering potential mechanisms of MeHg toxicity, the factors mediating a MeHg insult in the neuromuscular domain have not yet been fully identified and characterized.

Prior studies have attributed the MeHg-related motor deficits in children to effects on either the developing nervous system or musculature, rather than on the overall integrity of the neuromuscular system (Ekino *et al.*, 2007; Harada, 1995; Usuki *et al.*, 1998, 2001). Although acute MeHg exposure to mature neuromuscular junction (NMJ) preparations has been shown to reduce neurotransmission (Atchison and Narahashi, 1982), the effects of early life MeHg exposure on NMJ development and maintenance, which ultimately influences adult motor function, have not been thoroughly examined. Our prior study indicated that MeHg can simultaneously target the developing larval somatic muscles and the innervating motor neurons during Drosophila embryogenesis (Engel and Rand, 2014). We recently demonstrated that a targeted increase in Nrf2 antioxidant pathway activity in either developing muscles or motor neurons could partially rescue adult muscle morphogenesis and the eclosion behavior (emergence of the adult from the pupa casing) (Gunderson *et al.*, 2020), supporting the notion that MeHg may target specific muscle-neuron crosstalk events during development. The Drosophila model has served to establish fundamental cellular and molecular events in development, maturation, and maintenance of the neuromuscular system and NMJs. The adult indirect flight muscles (IFMs) share a homologous fibrillar structure and many developmental processes with vertebrate skeletal muscle (Fernandes *et al.*, 1991; Schulman *et al.*, 2015; Sink, 2006; Spletter *et al.*, 2018). The IFMs are therefore a particularly robust experimental model due to the genetic accessibility of these muscles and their motor neurons and the ability to relate developmental morphogenesis to behavioral phenotypes. The IFMs are required for flight and are composed of two muscle groups: the dorsal-longitudinal muscles (DLMs) and dorsoventral muscles (Swank, 2012). The IFMs are innervated by the embryonically derived intersegmental neuron (ISN) and segmental neuron (SN) (Fernandes and Vijayraghavan, 1993). The tightly choreographed development of the IFM fibers is essential for the outgrowth of primary nerites and formation of higher ordered branches of the ISN and SN, as well as the initial establishment of their NMJs (Fernandes and Vijayraghavan, 1993; Fernandes and Keshishian, 1998; Hebbar and Fernandes, 2004). In turn, the IFM fibers require their motor neurons for myoblast proliferation and migration, partial patterning formation, and muscle growth (Fernandes and Keshishian, 1998). The regulation and establishment of the neuromuscular system in Drosophila involves many types of conserved cell adhesion proteins, including the heterophilic binding partners neurexins (Nrx) and neuroligins (Nlg) (Sun and Xie, 2012). The Drosophila genome contains two *nrx* and four *nlg* genes that are highly homologous to the mammalian forms (Knight *et al.*, 2011; Tabuchi and Sudhof, 2002). Nrxs are predominantly localized to presynaptic active zone terminals, whereas Nlgs are localized to the post-synapse (Knight *et al.*, 2011). Drosophila *neuroligin 1* (*nlg1*) is the only neuroligin known to be expressed exclusively in muscle, whereas *nlg2-4* are widely expressed across post-synaptic neuron types and muscles (Banovic *et al.*, 2010; Poulopoulos *et al.*, 2009; Xing *et al.*, 2014; Zhang *et al.*, 2017). Together, Drosophila neurexin 1 (Nrx1) and Nlg1 form a trans-synaptic complex that regulates axonal arborization and NMJ morphology, maturation, and function (Banovic *et al.*, 2010; Chubykin *et al.*, 2007; Constance *et al.*, 2018; Knight *et al.*, 2011; Varoqueaux *et al.*, 2006; Xing *et al.*, 2018). The relative abundance of Nrx1 and Nlg1 across the motor-end plate is important for NMJ morphology and function. *Drosophila* mutants or transgenic knockdown of either *nrx1* or *nlg1* causes misalignment of synaptic machinery, perturbs synaptic activity, and severely limits NMJ growth and maturation (Banovic *et al.*, 2010).

Evidence from Caenorhabditis *elegans and Drosophila* implicates neuroligins in mediating mercury toxicity. Neuroligin-deficient *C. elegans* have reduced mean survival time following exposure to a mercury-containing compound, thimerosal, implicating that insufficient neuroligin expression is associated with a hypersensitivity to mercury exposure (Hunter *et al.*, 2010). Also, adult MeHg exposure reduced neuroligin-1 gene expression in the hippocampus of male BALB/c mice (Mellingen *et al.*, 2021). Furthermore, a previously conducted genome-wide association study (GWAS) in Drosophila identified *nlg1* as a developmental gene associated with MeHg sensitivity (Montgomery *et al.*, 2014).

Here, we leveraged the *Drosophila* model to characterize a role for muscle-specific Nlg1 to mediate MeHg insults in the developing neuromuscular system. We investigated the effects of MeHg exposure on IFM morphogenesis, innervation, and function via flight assays in concert with monitoring gene expression of *nlg and nrx* family members. The direct influence of Nlg1 and Nrx1 as mediators of MeHg toxicity was evaluated via targeted genetic manipulations in either a muscle-specific or neural-specific manner.

MATERIALS AND METHODS

Test substance. Methylmercury chloride was acquired from Sigma-Aldrich (no. 215465).

Drosophila stocks, GAL4>UAS System, and MeHg treatments. Transgene overexpression and RNAi hairpin-mediated knockdown of genes were performed using the GAL4>UAS system (Brand and Perrimon, 1993). The full list of fly strains used in this study with their corresponding purpose and source can be found in Supplementary Table 1. Generally, tissue-specific manipulations of gene expression utilized the GAL4 (G4) driver lines under the control of either muscle-specific promotor (eg, myocyte enhancer factor 2 [Mef2]) or neuron-specific promotor (VGlut [OK371] or RapGAP1 [OK6]). In Drosophila, all motor neurons are glutamatergic (Mahr and Aberle, 2006). Glutamatergic neurons are also located in most adult brain regions, indicating a role in controlling other processes outside of muscle contraction (Daniels *et al.*, 2008). The OK371-G4 drives in brain glutamatergic neurons and all motor neurons, whereas OK6-G4 is restricted to the motor neurons. Expression of *Keap1*, *nlg1*, and *nrx1* was modulated with the upstream activating sequence (UAS)-directed expression of the full-length gene for overexpression or the corresponding RNAi hairpin construct for knockdown of expression.

To block neurotransmission during various stages of IFM development and to assess IFM morphology, a temperature-sensitive mutant of the loss of function allele of Shibire (UAS-Shi[1]), a dynamin GTP-ase (Chen *et al.*, 1991; 1992), was expressed in glutamatergic neurons (OK371-G4, MHC-GFP) using the OK371-G4. This line also contains the myosin heavy chain (MHC) promoter controlling GFP production, such that the IFM can be visualized in live animals. Neurotransmission is blocked as a consequence of disrupted neurotransmitter recycling (Koenig and Ikeda, 1983, 1989). At permissive temperatures (22°C),

individuals expressing Shi[1] develop and behave normally. However, at nonpermissive temperatures (29°C), the Shi[1] protein fold shifts towards a nonfunctional conformation, inhibiting the reuptake of neurotransmitters and eventually leading to vesicle depletion, blocked neurotransmission, and paralysis (Koenig *et al.*, 1983). Targeted expression of Shi[1] acts in a dominant negative manner in the target tissue. Crosses and progeny were maintained at 22°C until shifted to 29°C to block neurotransmission at particular stages of IFM development. These induction phases were chosen to coincide with important processes of neuromuscular development: splitting of larval template cells and extensive axonal branching (12–20 hours after puparium formation [h APF]), myoblast fusion and establishment of adult innervation pattern (20–26 h APF), IFM fiber compaction and start of fiber elongation (26–34 h APF), and myotendinous junction and NMJ maturation (40–48 h APF). The staging of these events was based on literature (Fernandes and Vijayraghavan, 1993; Peppriell *et al.*, 2020; Spletter *et al.*, 2018) and our own observations. Following the 29°C induction phase, animals were transferred back at 22°C for the remainder of metamorphosis, eclosion, and adult stage leading up to flight tests to allow for normal neurotransmission to occur. IFM morphology was assessed at 60 h APF in all staged pupa and representative images were taken for each sample type. To ensure neurotransmission was inhibited as intended, eclosion ability (Rand *et al.*, 2014) was used as a readout of neurotransmission. Shifting animals expressing Shi[1] in glutamatergic neurons, which includes all motor neurons, to 29°C at the end of metamorphosis should block eclosion, as neurotransmission is required for eclosion. At 90 h APF, we shifted 60 control and Shi[1] animals to 29°C for 25 h and then counted the number of eclosed adults. For flight test, animals were kept at 22°C for 7 days post-eclosion (d PE).

The temperature-sensitive GAL80/GAL4>UAS system allows for temporally targeted alterations in gene expression. At noninduced temperatures (25°C), the GAL80 (G80) protein represses the G4 activity and prevents activation of the UAS sequence and downstream gene expression. At induced temperatures (29°C), the G80 repression is removed and the G4 transcription factor can active the UAS sequence and desired gene transcription. Temporally restricted knockdown of *nlg1* expression specifically in muscle during a window of IFM development (20–36 h APF) was achieved by using a Mef2-G4/Tublin-G80^{TS} construct in combination with a UAS-Nlg1$^{RNAi\ (KK)}$ construct. Animals were allowed to develop, eclose, and age to 7d PE at 25°C both prior and postinduction to ensure wildtype *nlg1* expression levels. The changes in gene expression were evaluated at 36 and 72 h APF, eclosion ability, and flight ability at 7d PE in response to the 20–36 h APF *nlg1* knockdown.

Developmental MeHg treatments were achieved by seeding first-instar larvae (L1) at a density of 50/vial into food (Jazz Mix, Fisher Scientific, no. AS153) containing 0, 2.5, 5, 10, or 15 μM MeHg, which is equivalent to 0, 0.5, 1, 2, and 3 ppm. In comparison, a serving of tuna or swordfish meant for human consumption can contain 0.3–3 ppm MeHg (Groth, 2010). MeHg exposure occurs during larval development and continues throughout metamorphosis as the pupal stage is a closed system and prevents the excretion of MeHg.

Staging. Pupae were staged according to the start of metamorphosis, deemed 0 h APF. Developmental timing associated with specific IFM innervation and morphogenesis events were obtained from Fernandes and Vijayraghavan (1993) and Spletter *et al.* (2018), respectively. All pupal ages, collection times, and induction times are reported as equivalent ages at 25°C. For experiments conducted at 22°C, pupal age was determined by the formula: h APF at 22°C × 0.67 = h APF at 25°C (Hummon and Costello, 1988). For accurate pupal staging, 0 h APF pupae were removed from vial using a damp paintbrush and placed on a microscope slide. The microscope slide was positioned in a covered 100 mm Petri dish with damp paper to maintain a humid environment and placed at the desired experimental temperature. Imaging or sample collection occurred once the pupa reaches the correct h APF. Recently eclosed adults were collected and separated into new vials every morning to accurately track their age in d PE.

Mercury analyses. Total mercury (tHg) body burden after MeHg dosing during larval stage was determined by three replicates of 5–10 pooled individuals of either pharate adults (approximately 90 h APF) or eclosed adults separated by sex. tHg was determined using the DMA-80 Direct Mercury Analyzer (Milestone, Connecticut) and determined in μg/g of wet weight and expressed as parts per million (ppm).

Imaging and phenotype quantification. To assess IFM morphology, pupae were dissected from the puparium at the designated developmental stage and placed dorsal side up on double-stick tape on a microscope slide. Pupae were lived imaged on Nikon AZ100 Multizoom microscope (MVI, Avon, Massachusetts). Within each experiment, at least 10 individuals were imaged with the most representative individual included in the figure.

Sh-GFP flies were used to assess adult IFM innervation pattern after larval MeHg exposure. Although the Sh-GFP construct allows for the visualization of the NMJ in larval somatic muscles, it is not well characterized in adult flight muscles. Sh-GFP L1 larvae were seeded onto 0 or 5 μM MeHg and allowed to develop at 25°C. At 10–13 days post-seeding, flies were transferred to fresh non-MeHg food. At 7d PE, male thoraxes were separated from other body regions with removal of wings and legs, fixed in methacarn (60% methanol [Fisher Chemical, no. A411], 30% chloroform [Fisher Bioreagents, no. BP1145], 10% glacial acetic acid [J.T. Baker, no. 9508-05]) for 4 h at room temperature, and then stored in 100% methanol at 4°C until tissue preparation. At room temperature with gentle shaking, thorax permeabilization comprised of two 20-min washes in 20% DMSO (Fisher Bioreagents, no. BP231) in methanol, one 20-min wash in 80% methanol in DI water, one 20-min wash in 50% methanol in 1X-PBS (SAFC, no. 56064C), two 20-min washes in 1X-PBS, and two 20-min washes in 1% Triton X-100 (ACROS Organics, no. 327372500) in 1X-PBS. Prepped thoraxes were positioned dorsal side up onto double stick on a microscope slide. A fresh scalpel was used to cut and bisect the thorax parallel to the DLMs to create two hemithoraxes. Hemithoraxes were blocked in 1:1 Aquablock (EastCoast Bio, no. PP82):1X-PBS for 1 h at 4°C, then incubated overnight at 4°C with primary antibodies. Primary antibodies include rabbit anti-GFP (Torrey Pines Biolabs, no. TP401) and mouse anti-Futsch (Developmental Studies Hybridoma Bank, no. 22C10) at a 1:300 and 1:25 dilution, respectively. Samples were washed 3 times in 1X-PBS for 5 min and then incubated for 1.5 h at 4°C with appropriate fluorescent-conjugated secondary antibodies, Alexa Fluor goat anti-mouse 647 (Fisher Scientific, no. A32728) and Alexa Fluor goat anti-rabbit 555 (Fisher Scientific, no. A21428). Hoechst nuclear stain was added the last 30 min of the secondary incubation. Samples were then washed 3 times in 1X-PBS for 5 min. Hemithoraxes were mounted with the sagittal aspect of the DLM fibers positioned upwards and oriented between two 1.5

cover slips (Fisherbrand, no. 12-541A) adhered to the microscope slide. A coverslip placed over the mounted samples is adhered in place with clear nail polish. The hemithoraxes were then flooded with Fluoroshield (Abcam, no. 104135) and nail polish was used to seal both ends. Hemithoraxes were imaged on the Nikon AZ100 microscope.

To quantify extent of DLM fiber innervation, the area stained of 22C10 antibody was measured. The single-channel images for 22C10-647 were imported to ImageJ (NIH) and converted to 16-bit images. A region of interest was drawn around the DLMs and all 22C10+ motor neurons such that the remaining portions of the image were excluded. The pixel threshold was manually adjusted using the Moments threshold setting. Measurement parameters included area, mean gray value, and area fraction with measurements being limited to threshold. The area fraction is represented as a percent and a minimum of 10 hemithoraxes were measured for each concentration. For the representative images, each fluorescent channel was pseudo-colored to maximize the contrast between the muscle fibers (pink) and the innervating motor neuron (green). The remaining male and female flies were used to conduct a flight assay at 7d PE.

Eclosion assay. Eclosion (emergence of the adult from the pupa case) is the very first neuromuscular event of the adult fly. MeHg tolerance of the various genotypes were assayed using the previously described eclosion assay (Mahapatra *et al.*, 2010; Rand *et al.*, 2014). Briefly, 50 L1 larvae/vial were seeded onto food (Jazz Mix, Fisher Scientific, no. AS153) containing 0–15 μM MeHg, and allowed to develop for 13 days at 25°C. Successfully eclosed flies were scored (maximum 150 flies) and expressed as percent of total larvae seeded. Each genotype was assessed on the various mercury conditions in triplicate. Viability eclosion assays were conducted using the above description except with the use of standard fly food containing no MeHg.

For eclosion experiments that staged pupae starting at 0 h APF, eclosion was assessed 1 day post the anticipated day of eclosion. Eclosion ability is the percent of empty pupa cases out of total number of pupa cases on one microscope slide. Three individual microscope slides were assessed for eclosion with at least 50 staged individuals.

Flight assay. Flies that successfully eclosed off 0, 2.5, or 5 μM MeHg in eclosion assays were placed onto fresh MeHg-free food starting at day 10 post-seeding and until day 13 when the eclosion assay was scored. Prior to testing, adult flies were separated by sex into groups of 25/vial 2 days prior to desired post-eclosion day age. After 48 h of CO_2 recovery, flies at 7 or 11d PE were tested for flight performance. Because mercury has a $t_{1/2}$ of roughly 7 days in adult flies (unpublished observation), conducting the flight assay at 7 or 11d PE allows for significant mercury clearance from the animals. Non-MeHg flight assays were conducted at 7d PE for consistency in age at time of testing across experiments. Flies were kept at 25°C during exposure, aging, and recovery periods. Flight tests were performed as described previously (Peppriell *et al.*, 2020). Briefly, flies were ejected into the flight cylinder by dropping one vial at a time through a drop column. The flight cylinder (76.2 cm in height) was lined with a removeable acrylic plastic sheet with paintable adhesive (TangleFoot Tangle-Trap Inc.) to capture flies on the sheet after they alighted once they entered the cylinder. Once all vials have been dropped, the plastic sheet was removed, placed in front of a white background, and imaged for digital quantification via WebPlotDigitizer software. Landing height of each individual fly is represented in centimeters (cm) and corresponds to that individual's flight ability. Flies that fell to the bottom of the flight cylinder and collected in a mineral oil dish was categorized as "flightless" and given the lowest landing height of 76.2 cm. Summary data of each flight test is provided in the Supplementary Material.

Rt-qPCR. Alterations in relative gene expression due to transgenic gene manipulations or MeHg exposure were determined by quantitative reverse transcriptase PCR (RT-qPCR) using the $2^{-\Delta\Delta Ct}$ method (Livak and Schmittgen, 2001). Each biological replicate represents total RNA isolated from an independent pooling of 10 staged whole-body pupae or adult body region. Adult body regions were collected by separating the head, thorax, and abdomen using a clean razor blade. RNA was extracted using Trizol and chloroform (Fisher Scientific, no. BP1145-1). Total RNA was converted to cDNA using the High Capacity cDNA Reverse Transcription Kit (Applied Biosystems, no. 4368813), according to manufacturer's protocol. RT-qPCR was completed using iTaq Universal SYBR Green Supermix (Bio-Rad, no. 1725121) with forward and reverse primers specific for genes of interest (Supplementary Table 2) on a Bio-Rad CFX96 Real-Time PCR system, both according to manufacturer's instructions. Normalization of inter-samples mRNA levels was performed using ribosomal protein RP49 as a reference housekeeping gene (Deng and Kerppola, 2013; Teng *et al.*, 2012).

Statistical analysis. All statistical analyses were completed in JMP Pro 15. Comparisons of treatment group or experimental genotypes were evaluated in relation to the relevant untreated group or genotype control, as indicated. For eclosion assays, rates of eclosion for indicated strains at each heat pulse induction phase or MeHg exposure are expressed in proportions (% eclosion). Most assays were performed to achieve a sample size of at least 150. Statistical consideration of differences between experimental and control fly strains are therefore comparisons of proportion values and not of continuous values. Because error determinations in proportion values become restricted at the edges (ie, near 0% and 100%), an analysis of variance (ANOVA) was not used. Statistical analyses of eclosion assays were therefore done using a pairwise 2-tailed z test, categorically comparing each treatment with control. For flight assays, 1- or 2-way AVOVAs were used to evaluate landing heights between treatment, genotype, and/or sex, where appropriate. Counts of Shi[1]-induced IFM perturbation was analyzed by 2-tailed Fisher's Exact test between genotypes of the same induction phase. All gene expression levels with temporal-restricted knockdown of *nlg1* were normalized to w1118 at 36 h APF, but 1-way ANOVA tests occurred between groups within the same timepoint (either 36 or 72 h APF). Statistical significance by 1- or 2-way ANOVA is indicated by the letter system employed by the JMP software. Significance between 2 groups is demonstrated when there is different letter(s) for each data group. If a single letter is the same between 2 groups, then those 2 groups are not statistically significant. All experiments or sample collections were conducted in independent, biological triplicates. Data presented as mean ± standard error. In all cases, significance was defined as $p \leq .05$.

RESULTS

Requirement for Neurotransmission in IFM Development

Development of a functional neuromuscular unit for flight relies on coordinated morphogenesis of the IFMs and their cognate motor neurons. However, the extent to which developing muscles versus their neuronal partners are susceptible to MeHg

Figure 1. Neurotransmission is required during early IFM development for proper morphogenesis and adult function. A, Experiment schematic detailing various induction phases across pupal development and corresponding ages of IFM morphology, eclosion ability, and flight ability assessment. B, Summary data detailing the impacts of Shi[1] inhibition in glutamatergic neurons (OK371-G4, MHC-GFP) across pupal development on IFM morphology and eclosion ability. Frequency of IFM dysmorphology with Shi[1] animals was compared with genotype controls (>w1118) of the same induction phase ($n \geq 145$ pupae/induction phase/genotype, $^{*}p < .5$, 2-tailed Fisher's Exact test). Eclosion ability was measured as an output of neuromuscular function ($n \geq 60$ pupae/induction phase/genotype, $^{*}p < .05$, Z test). C–L, Representative images of w1118 and Shi[1] 60 h APF IFM morphology after various induction phases. J, Thinner DLMs (white arrow) caused by inhibition of neurotransmission via induction of Shi[1] between 26 and 34 h APF. Landing height of 7d post eclosion (PE). (M) males and (N) females with neurotransmission inhibited across different pupal developmental stages ($n \geq 50$ individuals/induction phase/genotype/sex, mean ± SEM, $p < .05$, 2-way ANOVA with Tukey's post hoc, significant differences indicated by different letter labels).

remains to be explored. Thus, we first sought to understand the reliance of the developing IFM on functional neurotransmission between the forming muscle and its innervating neurons. To achieve this, we attempted to block neurotransmission presynaptically, specifically at the level of the motor neuron, at different stages of IFM development and assess effects on IFM morphology and function. The Shibire[1] mutant (Shi[1]) encodes a temperature-sensitive loss of function allele of a dynamin GTP-ase, which has previously been used to implement ubiquitous cessation of endocytosis, including synaptic vesicle recycling. Thus, an effective loss of neurotransmission is achieved by implementing a heat pulse (29°C) to flies (Koenig and Ikeda, 1983, 1989; Koenig *et al.*, 1983). A prior study using Shi[1] flies showed that a heat pulse from 20 to 26 h APF greatly disrupts IFM morphogenesis and muscle function in eclosion (Hummon and Costello, 1988). Heat induction at other times, such as 44–50 h APF, have no effect on IFM morphology (Hummon and Costello, 1988), highlighting a potential developmental window of sensitivity. However, the Shi[1] phenotype cannot be attributed solely to blocking neurotransmission as IFM development itself requires endocytic recycling (Hummon and Costello, 1993). Here, we leveraged a UAS-Shi[1] construct to achieve a dominant-negative suppression of endocytic recycling restricted to all motor neurons including those that innervate the IFMs. Because all Drosophila motor neurons are glutamatergic neurons we restricted Shi[1] expression using a glutamatergic neuron-specific driver (OK371-G4>UAS-Shi[1], MHC-GFP). By blocking neurotransmission presynaptically at 26–34 h APF (see Figure 1A) we observed a significant perturbation in IFMs, characterized as thinner DLM fibers (white arrow in Figure 1J), albeit occurring at a low frequency (3.48%, Figure 1B). Remarkably, heat pulse in other windows failed to influence IFM morphology (Figs. 1C–H and L). Importantly, eclosion was completely inhibited following Shi[1] induction spanning 90–114 h APF, the window leading up to eclosion (Figure 1B), confirming the efficacy of the OK371-G4>UAS-Shi[1] construct and the role of glutamatergic neurons in eclosion. However, eclosion was not impaired with heat pulses administered during earlier developmental timepoints (Figure 1B). Motor neuron restricted Shi[1] induction within the 26–34 h APF window also led to deficits in adult flight function in both males and females at 7d PE (Figs. 1M and N). No effects on flight were observed when Shi[1] was induced in other developmental windows (Figs. 1M and N). Together, these results indicate the functional necessity of the NMJ during the 26–34 h APF window of IFM development for subsequent adult function.

Developmental MeHg Exposure Reduces Adult DLM Innervation

The integrity of the adult neuromuscular unit was assessed following developmental MeHg exposure. The motor neuron that serves the DLM was visualized using the microtubule-associated

Figure 2. Developmental MeHg exposure reduces adult DLM innervation. A, General schematic of neuromuscular architecture of IFM and the innervating motor neuron. Representative images of hemithoraxes showcasing the extent of DLM innervation in developmentally (B) untreated or (C) 5 μM MeHg-treated 7d PE male adult visualized with 22C10 antibody (motor neurons), and Hoechst (nuclei). The adult trachea is indicated by "T". D, Quantification of 22C10 area stained as a measure for degree of DLM innervation ($n \geq 10$ hemithoraxes/treatment, mean ± SEM, $^*p < .05$, Student's *t* test). E, Male (circle) and female (square) landing height at 7d PE with or without developmental treatment of 5 μM MeHg ($n \geq 49$ individuals/treatment/sex, mean ± SEM, $^*p < .05$, Student's *t* test, comparison within same sex).

protein and axonal marker Futsch (22C10 antibody) in 7d PE adult flies carrying the shaker reporter gene (Sh-GFP) intended to reveal the NMJs. Hoechst stain was used to reveal the nuclei and the outline of the myofibers. The Sh-GFP expression failed to reveal discernable adult NMJs (data not shown). Nevertheless, the 22C10 signal afforded the opportunity to assess the broader impact of developmental MeHg on adult ISN and SN innervation pattern. Compared with untreated controls, the extent of the innervation of the DLM was reduced following developmental MeHg exposure (Figs. 2B–B″, C–C″, and D), as was the typical expanse of motor neuron branching across the DLM fibers (Figs. 2B–B′ and C–C′). The reduction in DLM innervation paralleled decrements in flight performance in both males and females (Figure 2E). Gross effects on adult DLM muscle morphology were not observed at 5 μM MeHg treatment (Figs. 2B″ and C″). The incomplete elaboration and stabilization of motor axon extensions in adults are consistent with the notion that developmental MeHg may disrupt NMJ establishment and maturation, which results in a subsequent flight function deficit.

Muscle- Versus Motor Neuron-Specific Contribution to MeHg-Induced Flight Deficits

We next assessed the effects of MeHg on muscle and neuron development to ascertain the relative contribution of each to exposure-related functional deficits in flight. Flight assays were conducted on 7d PE male and female flies with either muscle- (Mef2-G4) or motor neuron-specific (OK6-G4) modulation of MeHg "protection" via targeted elevation or reduction in Nrf2 activity through *Keap1* overexpression or knockdown. Our prior work demonstrated that upregulation of Nrf2 signaling via knockdown of *Keap1*, the negative regulator of Nrf2, can rescue MeHg effects on IFM development and eclosion (Gunderson *et al.*, 2020). In genotype controls (>w1118) of both sexes, developmental MeHg exposure induced a dose-dependent decrease in landing height at 7d PE (Figs. 3A and B). In untreated controls, muscle-specific *Keap1* overexpression to inhibit Nrf2 activity dramatically reduced landing height in both male and female 7d PE flies, with developmental MeHg exposure yielding no further reduction (Figs. 3A and B). However, muscle-specific *Keap1* knockdown (>Keap1^{RNAi}), which moderately activates Nrf2 signaling, significantly rescues flight ability in both males and females at 2.5 and 5 μM MeHg, seen by an increase in landing height compared with controls at the same exposure (Figs. 3A and B). In parallel, the tHg body burden was measured in late pupae (approximately 90 h APF) and adults at the time of the flight assay to assess if differential effects in landing height were related to a lower accumulation of the MeHg dose (Figs. 3C–E). Across all stages and genotypes, tHg was constant within each sex; the rescue in flight ability with *Keap1* knockdown

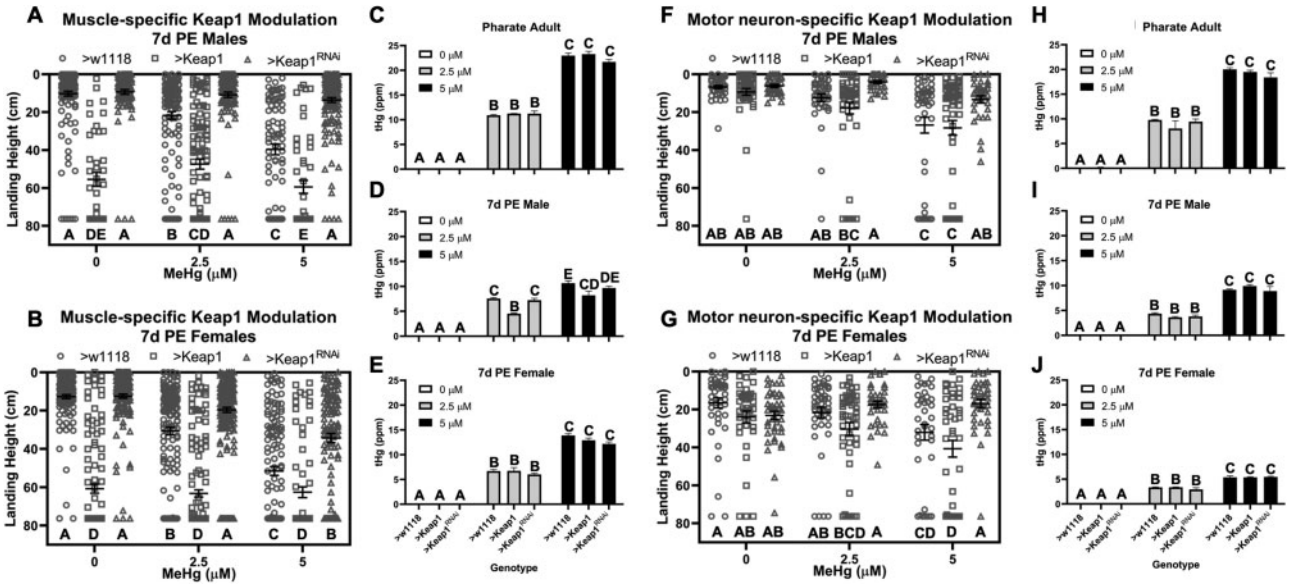

Figure 3. Muscle and motor neuron-specific activation of Nrf2 pathway rescues flight ability. (A) Male and (B) female landing height at 7d PE with muscle-specific (Mef2-GAL4) *Keap1* overexpression (square) or *Keap1* knockdown (triangle) compared with genotype control (circle) after developmental exposure to 0, 2.5, or 5 μM MeHg ($n \geq 42$ individuals/genotype/treatment/sex, mean ± SEM, $p < .05$, 2-way ANOVA with Tukey's post hoc, significant differences indicated by different letter labels). tHg body burden of (C) pharate adults (approximately 90 h APF). (D) 7d PE males and (E) 7d PE females with muscle-specific *Keap1* overexpression or knockdown compared with genotype controls ($n = 3$ samples/genotype/treatment, mean ± SEM, $p < .05$, 2-way ANOVA with Tukey's post hoc, significant differences indicated by different letter labels). (F) Male and (G) female landing height at 7d PE with motor neuron-specific (OK6-GAL4) *Keap1* overexpression (square) or *Keap1* knockdown (triangle) compared with genotype control (circle) after developmental exposure to 0, 2.5, or 5 μM MeHg ($n \geq 30$ individuals/genotype/treatment/sex, mean ± SEM, $p < .05$, 2-way ANOVA with Tukey's post hoc, significant differences indicated by different letter labels). tHg body burden of (H) pharate adults (approximately 90 h APF). (I) 7d PE males and (J) 7d PE females with motor neuron-specific *Keap1* overexpression or knockdown compared with controls ($n = 3$ samples/genotype/treatment, mean ± SEM, $p < .05$, 2-way ANOVA with Tukey's post hoc, significant differences indicated by different letter labels).

is not attributed to a lower-body burden during metamorphosis or at time of testing (Figs. 3C–E).

We next evaluated motor neuron-specific *Keap1* knockdown, where flight ability is also rescued in both males and females at 5 μM MeHg (Figs. 3F and G). Motor neuron-specific *Keap1* overexpression did not itself influence flight ability and MeHg-related flight deficits were exacerbated at 5 μM MeHg in 11d PE, but not 7d PE, adults (Figs. 3F and G and Supplementary Figs. 1A and B). Across all genotypes, the tHg body burden was fairly constant within each sex in both 7 and 11d PE adults, indicating that the rescue in flight ability *Keap1* knockdown in neurons cannot be attributed to a reduced body burden of Hg (Figs. 3H–J and Supplementary Figs. 1C and D).

MeHg Selectively Represses nlg1 *Expression During Pupal Metamorphosis*

We next sought to identify factors that could mediate the MeHg-related loss of neuromuscular flight function. Our previous GWAS for MeHg susceptibility genes identified several candidates involved in various aspects of NMJ development (Montgomery *et al.*, 2014), including *nlg1*. The developmental timeline of NMJ formation during metamorphosis in Drosophila is illustrated in Figure 4A. Gene expression levels of *nlg1-4 and nrxs1*, 4 were first assessed at the time of adult innervation pattern establishment, 24 h APF (Fernandes and Vijayraghavan, 1993; Spletter *et al.*, 2018). Remarkably, MeHg selectively reduced *nlg1* expression in a dose-dependent manner (Figure 4B) at the 24 h APF timepoint. In contrast, MeHg did not influence the expression of *nlg2*, *nlg3*, *nlg4*, *nrx1*, or *nrx4* at 24 h APF. We next explored the impact of 10 μM MeHg on expression of these genes across metamorphosis relative to untreated controls at 0 h APF (Figs. 4C–G). Following developmental exposure to 10 μM MeHg, *nlg1* expression was reduced from 20 to 36 h APF, followed by an increase in expression at 72 h APF (Figure 4C). Interestingly, *nlg2*, *nlg3*, and *nrx1* expression levels were not changed by 10 μM MeHg in the 20–36 h APF window, yet expression of each gene was elevated at 72 h APF. Expression of *nlg3 and nrx1* in exposed groups was elevated at both 48 h and 90 h APF (Figs. 4D–F); this latter increase suggesting a compensatory elevation to earlier (20–36 h APF) suppression of *nlg1* (Figure 4C). Gene expression of *nrx4* was not affected by 10 μM MeHg at any timepoint assessed (Figure 4G).

Developmental MeHg Exposure Invokes Persistent Changes in NMJ Gene Expression in Adults

The persistence of the MeHg-related gene expression changes in *nlg1*, *nlg2*, *nlg3*, and *nrx1* was next assessed across adulthood during 1, 7, and 11d PE timepoints. Following developmental exposure 0 or 5 μM MeHg, gene expression of *nlg1*, *nlg2*, and *nlg3* from dissected thoraxes of adult flies exibited a characteristic rise and fall trend of expression across days 1 to 11, with an approximately 2-fold increase at day 7 (Figs. 5A–C and E–G). In contrast, *nrx1* showed a steady expression with a moderate decline at day 11. Remarkably, gene expression of *nrx1*, as well as *nlg1, nlg2*, and *nlg3* was reduced at most timepoints in groups exposed to MeHg during development relative to untreated control animals (Figs. 5A–H). Overall, these global changes in NMJ gene expression suggest that the maintenance, integrity, and function of the adult NMJ is compromised by a MeHg exposure at an earlier point during development.

Nlg1-Specific Effects on IFM Morphology and Flight Ability

We next explored whether the MeHg-induced *nlg1* expression reduction in the pupal stage could subsequently dysregulate other *nlg/nrx* family members later in development. Prior evidence in Drosophila embryos shows *nlg1* is expressed in

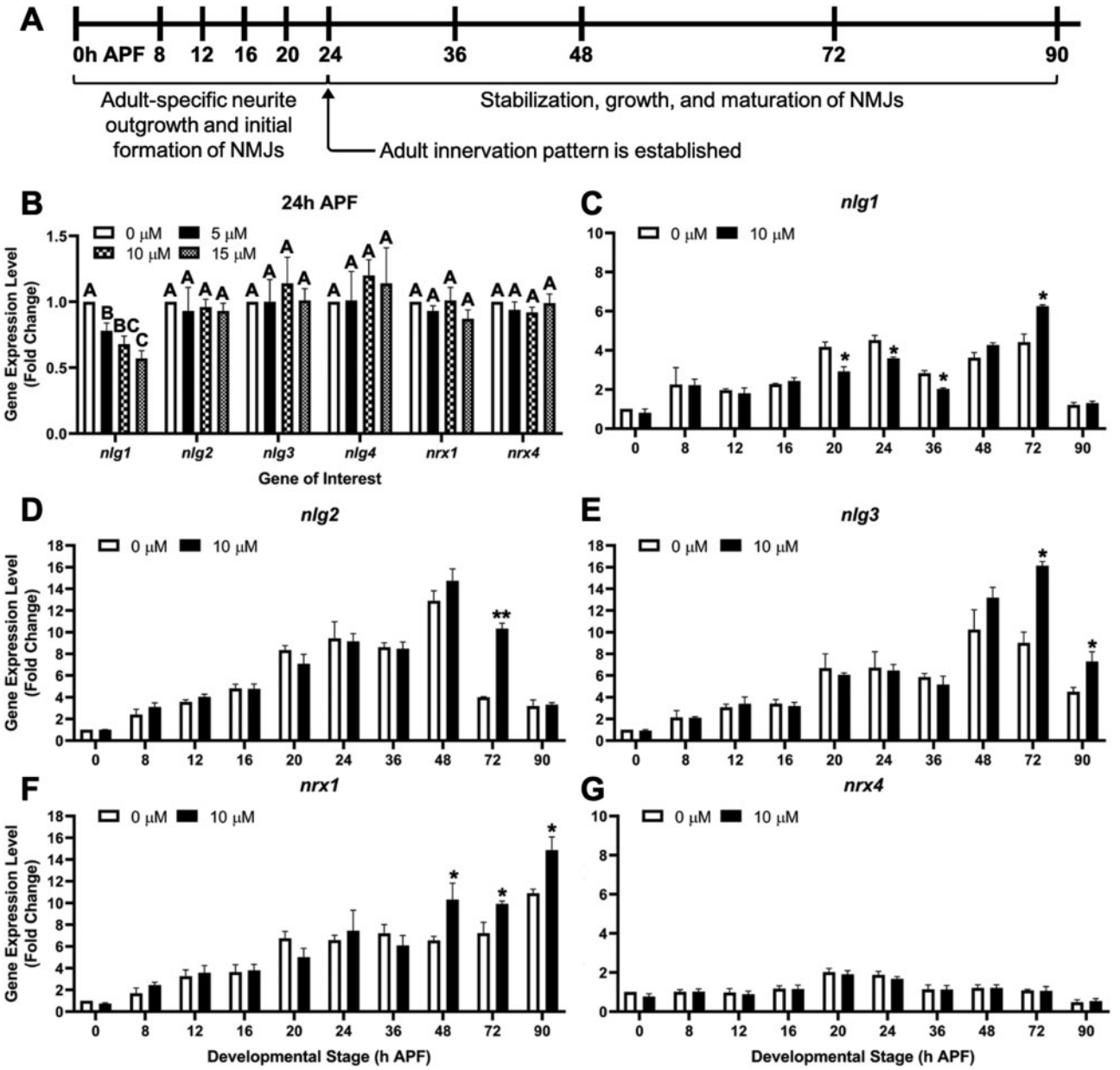

Figure 4. MeHg suppresses *nlg1* expression early in pupal development. A, Schematic pairing RNA collection time points with broad developmental neuromuscular events, with 24 h APF representing a major transition point. B, Gene transcript levels at 24 h APF for *nlg1*, *nlg2*, *nlg3*, *nrx1*, and *nrx4* with developmental exposure to 0, 5, 10, or 15 μM MeHg. For each gene, each concentration is normalized to untreated controls ($n = 3$, mean ± SEM, $p < .05$, 1-way ANOVA with Tukey's post hoc, significant differences indicated by different letter labels). Gene transcript levels with or without 10 μM MeHg for (C) *nlg1*, (D) *nlg2*, (E) *nlg3*, (F) *nrx1*, and (G) *nrx4* at selected developmental time points. Each data point is normalized to untreated, 0 h APF control gene expression ($n = 3$, mean ± SEM, $^{*}p < .05$, $^{**}p < .01$, Student's *t* test, compared with untreated control of same time point).

muscles whereas *nrx1* is restricted to neurons (Banovic *et al.*, 2010; Knight *et al.*, 2011). Therefore, we attempted to modulate expression of *nlg1* or *nrx1* alternately in either muscle (Mef2) or motor neurons (OK6) to compare effects on subsequent eclosion and flight behaviors (Figure 6). We first validated the specificity of *nlg1 and nrx1* expression to muscle and neurons, respectively. The Gal4 > UAS expression system was used to express RFP under the control of the regulatory gene sequences for *nrx1* (Nrx1 > RPF) or *nlg1* (Nlg1 > RFP), which revealed a definitive pattern of *nrx1* expression restricted to the central brain and eyes in the head and *nlg1* expression in the IFMs of pupae (Figs. 6A and B). In parallel, *nrx1 and nlg1* RNA transcript expression were measured in the head and thorax body regions of 1d PE adults. In both males and females, expression of *nrx1* in neurons was enriched, reflected by a lower ΔCt value of *nrx1* in the head (black bar) than in the thorax (white bar) (Figure 6C). In contrast, *nlg1* was more enriched in the thorax than the head in both male and female adults, consistent with IFM localization of *nlg1* (Figure 6C).

To assess the influence of muscle-restricted modulation of *nlg1 and nrx1* on IFM morphology in live pupae, we used the Mef2-RFP-G4 driver to knockdown or overexpress *nlg1 and nrx1* (Figs. 6D–J). In most cases, altered expression of *nlg1* or *nrx1* did not perturb IFM morphology. However, when a more robust 20-fold *nlg1* muscle-specific overexpression was achieved (Figure 6M), the DLM fibers were thinner (white arrow) and the TDT jump muscles (white asterisks) were missing (Figure 6H). Although eclosion ability was not

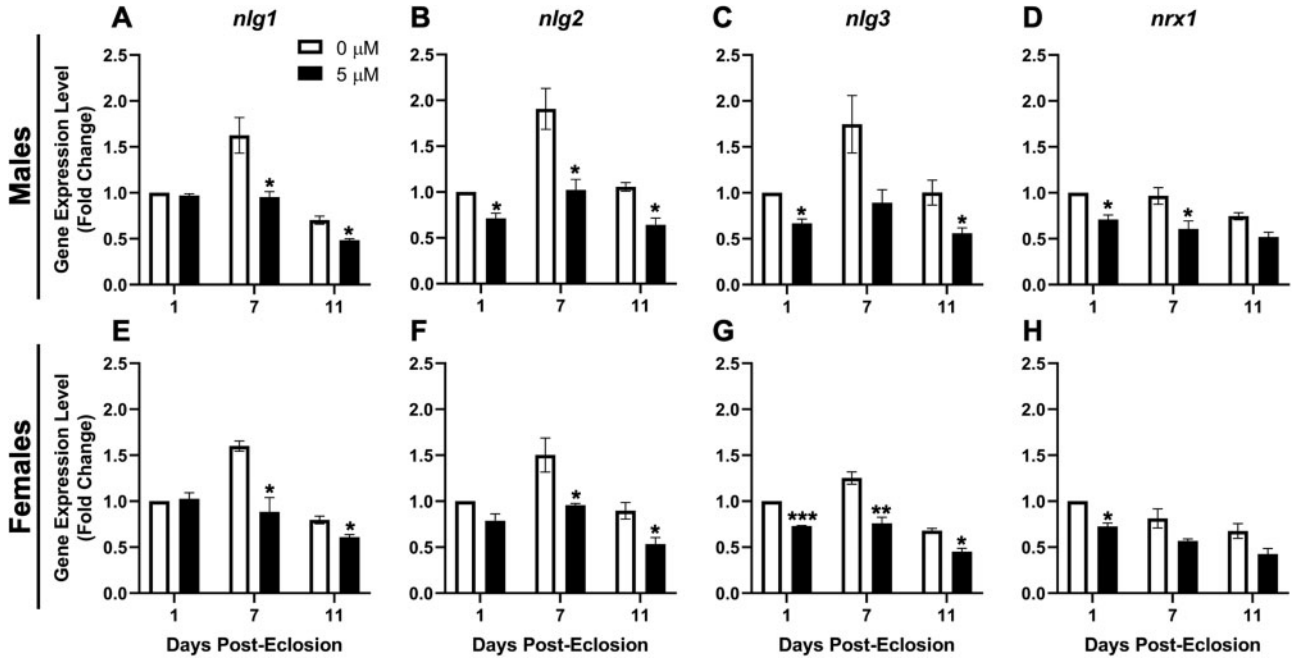

Figure 5. Developmental MeHg exposure alters adult NMJ factor gene expression. Gene transcript from pooled male or female thoraxes at 1, 7, or 11d PE for (A, E) *nlg1*, (B, F) *nlg2*, (C, G) *nlg3*, (D, H) *nrx1*, respectively, after developmental exposure to 5 μM MeHg. Data points are normalized to untreated, 1d PE gene expression within each sex ($n = 3$ pooled thoraxes/treatment/age/sex, mean ± SEM, $^{*}p < .05$, $^{**}p < .01$, $^{***}p < .001$, Student's *t* test, compared with untreated control of same age).

impacted by muscle-specific alteration in *nlg1* or *nrx1* (Figure 6K), adult flight ability was impaired (Figure 6L). Following *nlg1* knockdown to 50% of control levels (>Nlg1$^{RNAi\ (KK)}$), landing height was significantly reduced compared with controls (>w1118) in both male and female flies (Figure 6L). Curiously, a compensatory increase in *nrx1* was observed following *nlg1* knockdown to 50% of control levels with a second strain (>Nlg1$^{RNAi\ (GD)}$), which coincided with no effect on flight function (Figs. 6L and M). Overexpression of *nlg1* reduced flight function when expressed at higher levels (>Nlg1-GFP vs > Nlg1, Figs. 6L and M). In contrast, ectopic expression of *nrx1* (>Nrx1-GFP) in muscles did not influence flight function despite 30-fold induction (Figs. 6L and M). Nrx1 RNAi knockdown did not influence *nrx1* levels, further supporting that *nrx1* is not appreciably expressed in muscles (Figure 6M).

We next modulated *nlg1 and nrx1* expressly in motor neurons using the OK6-G4 driver (Figs. 6N–P). Whereas neither upregulation nor knockdown of *nlg1* or *nrx1* influenced eclosion ability (Figure 6N), male and female flight function was reduced by knockdown of *nrx1* in motor neurons (OK6>Nrx1$^{RNAi\ (GD2)}$) compared with control flies (>w1118) (Figure 6O). The approach reduced *nrx1* expression without affecting *nlg1* (Figure 6P). In contrast, gene expression of *nlg1* was elevated following *nrx1* knockdown in motor neuron (>Nrx1$^{RNAi\ (GD1)}$), despite no alterations in flight ability (Figs. 6O and P), suggesting a compensatory increase in *nlg1*. Targeted knockdown of *nlg1* in motor neurons (OK6 > Nlg1$^{RNAi\ (KK)}$) did not impact flight ability nor affect *nlg1 and nrx1* expression (Figs. 6O and P). Similarly, overexpression of *nlg1* (>Nlg1-GFP, > Nlg1) or *nrx1* (>Nrx1-GFP) in motor neurons did not affect flight function (Figs. 6O and P). Overall, these results demonstrate that IFM morphology and flight function are particularly sensitive to *nlg1* levels in muscles.

Targeted nlg1 *Knockdown at 20–36 h APF Partially Recapitulates MeHg Influence on NMJ Gene Expression and Flight Ability*

It was possible that the MeHg-induced reduction in *nlg1* gene expression during 20–36 h APF mediated the elevation in *nlg2*, *nlg3*, and *nrx1* expression later during pupal metamorphosis, as well as the adult-specific deficits in flight ability. To explore this possibility, the temperature-sensitive Mef2-G4, Tub-G80^{TS} system was applied to temporally induce *nlg1* knockdown (>Nlg1$^{RNAi\ (KK)}$) in developing muscles (Figure 7A). Gene expression at 36 and 72 h APF was assessed to confirm knockdown and recovery. After 16 h of induction, a 20% knockdown in *nlg1* was observed in 36 h APF pupae expressing RNAi hairpin for *nlg1* (Figure 7B). Upon recovery at 25°C for another 16 h, 72 h APF pupae *nlg1* levels had normalized back to control levels (Figure 7B). The initial suppression of *nlg1* did not influence gene expression of *nlg2*, *nlg3*, and *nrx1* at 36 h APF (Figs. 7C–E). However, at 72 h APF the expression of *nlg2*, *nlg3*, and *nrx1* was increased compared with 72 h APF controls, suggesting a compensatory mechanism (Figs. 7C–E). Eclosion ability was not altered with temperature or *nlg1* knockdown (data not shown). In males, there was a trending reduction in landing height in flies that had temporal 20–36 h APF *nlg1* knockdown (Figure 7F), and a significant decrease in landing height in the flies that actually flew (Figure 7G). In females, flight ability was not impacted by temporal developmental *nlg1* knockdown (Supplementary Figure 2). Overall, transgenic *nlg1* knockdown during a specific window of IFM development partially recapitulates MeHg effects on *nlg/nrx* gene expression in pupae and subsequent adult flight ability, further supporting that *nlg1* expression level between 20 and 36 h APF is especially important for proper development and function of the IFM.

Nlg1 Rescue of MeHg Developmental Toxicity in Eclosion and Flight Function

We next sought to rescue neuromuscular function by genetically compensating for MeHg suppression of *nlg1* expression. Eclosion ability was determined following MeHg exposure in combination with moderate (Mef2 > Nlg1-GFP) or strong (Mef2 > Nlg1) *nlg1* overexpression in developing muscle (Figs. 8A and B). Exposure to 5 or 10 μM MeHg in combination with moderate *nlg1* overexpression rescued eclosion ability compared with controls (Mef2 > w1118) of the same treatment (Figure 8A). The

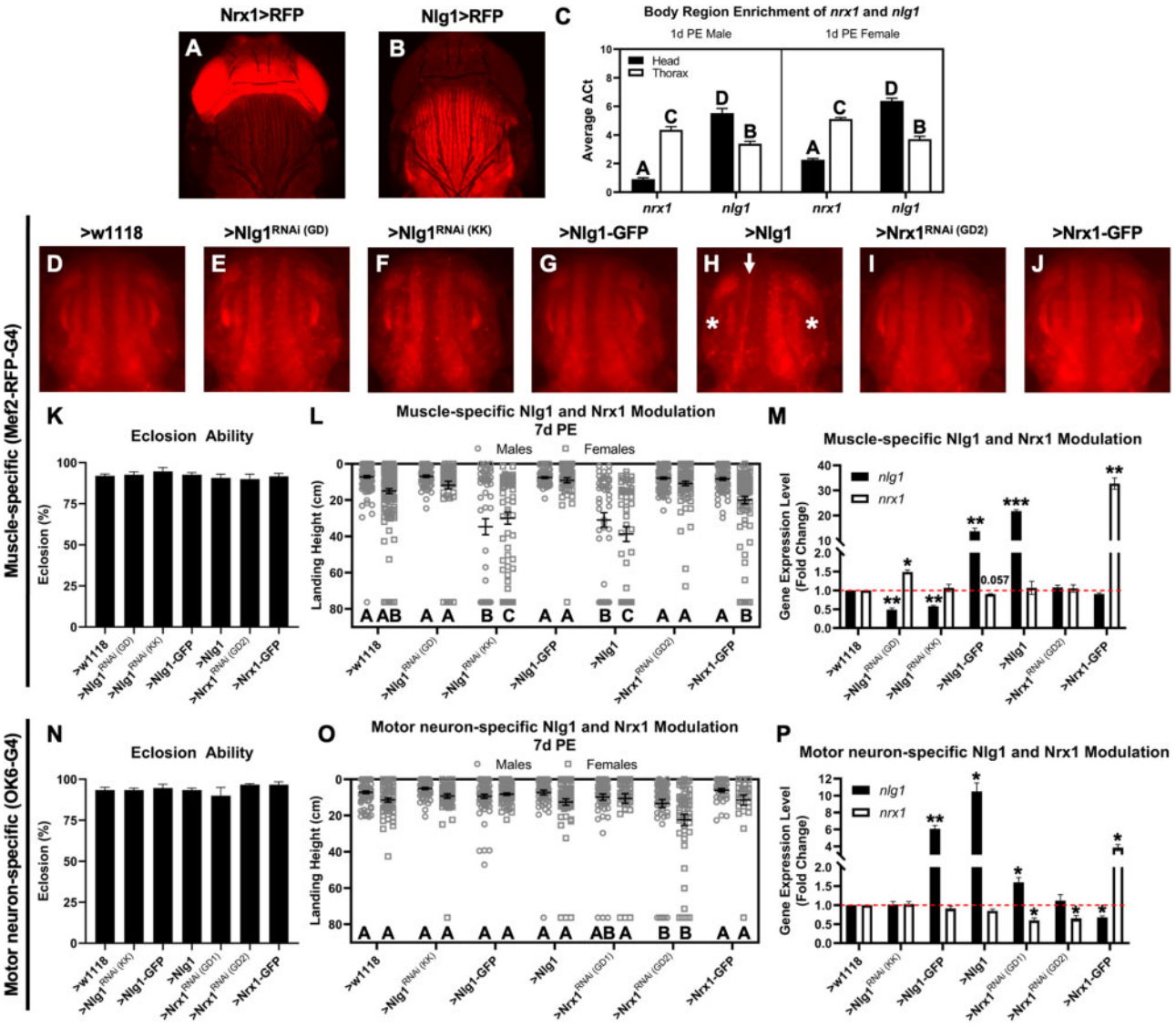

Figure 6. *nlg1 and nrx1* expression and activity is restricted to specific tissues constituting the motor unit. Expression of RFP fluorescent reporter under the control of (A) Nrx1-G4 or (B) Nlg1-G4 gene regulatory sequences for visualization of *nrx1 and nlg1* expression domain during pupal development. C, Delta Ct levels of *nrx1 and nlg1* in either head or thorax of 1d PE male or female wild-type flies ($n = 3$ samples/body region/sex, mean ± SEM, $p < .05$, 2-way ANOVA with Tukey's post hoc, significant differences indicated by different letter labels). D-J, Representative images of IFM morphology with muscle-specific (Mef2-RFP-G4) overexpression or knockdown of *nlg1* or *nrx1*. H, Strong muscle-specific *nlg1* overexpression induces thinner DLM fibers (white arrow) and missing TDT jump muscles (white asterisks). Eclosion ability with (K) muscle-specific (Mef2-RFP-G4) or (N) motor neuron-specific (OK6-G4) overexpression or knockdown of *nlg1* or *nrx1* ($n = 3$, mean ± SEM, Z test). Male (circle) and female (square) landing height at 7d PE with (L) muscle-specific or (O) motor neuron-specific overexpression or knockdown of *nlg1* or *nrx1* ($n \geq 27$ individuals/genotype/sex, mean ± SEM, $p < .05$, 1-way ANOVA with Tukey's post hoc within each sex, significant differences indicated by different letter labels). Whole pupal gene transcripts levels for *nlg1 and nrx1* with (M) muscle-specific or (P) motor neuron-specific overexpression or knockdown of *nlg1* or *nrx1*. For each gene, each genotype is normalized to the control expression level (>w1118) ($n = 3$, mean ± SEM, $^{*}p < .05$, $^{**}p < .01$, Student's *t* test, each genotype is compared with >w1118 expression levels).

combination with strong muscle-specific *nlg1* overexpression exacerbated eclosion deficits compared with controls; fewer adults eclosed at 5 and 10 μM MeHg (Figure 8B). Body burden of tHg in pharate adults was not impacted by genotype (Supplementary Figure 3A). Flight ability was next examined in 7 and 11d PE flies that successfully eclosed on 0, 2.5, and 5 μM MeHg. For both ages and in both sexes, 5 μM MeHg exposure led to flight deficits that were rescued by moderate overexpression of *nlg1*, indicating that muscle-specific *nlg1* overexpression can rescue IFM development and neuromuscular function from MeHg (Figs. 8C and D and Supplementary Figs. 3D and F). The body burden of tHg was not different between genotypes (Supplementary Figs. 3B, C, E, and G). Flight ability was also examined in adults following *nlg1* overexpression in motor neurons (OK6-G4). Flight ability at 7d PE was not rescued at any MeHg concentration when *nlg1* overexpression is targeted to developing motor neurons (Figs. 8E and F). Thus, the rescue potential of *nlg1* is specific to developing muscles.

DISCUSSION

In this study, we identified a muscle-specific factor, Nlg1, as a partial mediator of MeHg toxicity to neuromuscular function. Nlg1 is required for the proper establishment and function of the adult neuromuscular system (Constance *et al.*, 2018). We used a Shi[1] temperature-sensitive mutant to determine that

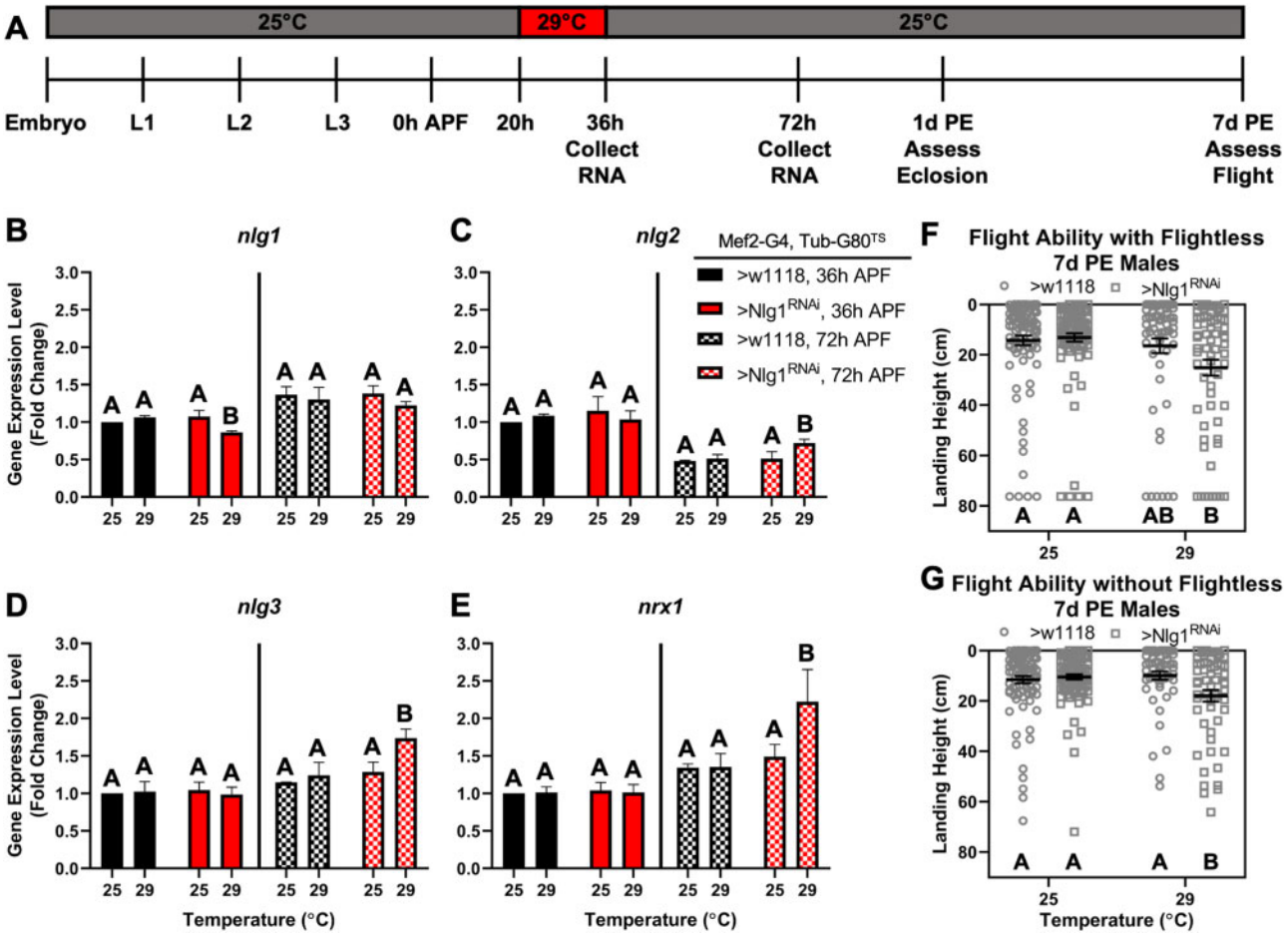

Figure 7. Temporally restricted *nlg1* knockdown partially recapitulates MeHg influence on gene expression and flight ability. A, Schematic outlining temporally restricted knockdown of *nlg1* between 20 and 36 h APF and time points for RNA collection and assessment of neuromotor behaviors of eclosion and flight. Gene expression fold changes for genotype controls (>w1118, black bars) and *nlg1* knockdown (>Nlg1^{RNAi}, red bars) at 36 h APF (solid bars) and after 16 h of recovery at 72 h APF (checkered bars) for (B) *nlg1*, (C) *nlg2*, (D) *nlg3*, and (E) *nrx1*. All data genotypes and time points are normalized to 36 h APF, 25°C gene expression ($n = 3$ samples/genotype/temperature/age, mean ± SEM, $p < .05$, 2-way ANOVA with Tukey's post hoc within each sex, significant differences indicated by different letter labels). Landing height of 7d PE males with or without *nlg1* knockdown between 20 and 36 h APF, (F) including or (G) excluding flightless ($n \geq 51$ individuals/genotype/temperature, mean ± SEM, $p < .05$, 2-way ANOVA with Tukey's post hoc within each sex, significant differences indicated by different letter labels).

IFM morphogenesis and adult function require neurotransmission at a specific window of development, during which NMJ function is essential. When neurotransmission was inhibited from 26 to 34 h APF, thinner, less developed DLM fibers were observed at 60 h APF and flight function was reduced during adulthood. Interestingly, developmental exposure to MeHg also suppressed *nlg1* expression within the 20–36 h APF window of development and led to latent reductions in adult flight function. Muscle-specific knockdown of *nlg1* from 20 to 36 h APF recapitulates MeHg and Shi[1]-induced flight deficits. Reductions in *nlg1* expression have been shown to inhibit NMJ maturation and decrease synaptic activity (Banovic *et al.*, 2010); our findings support the notion that the 20–36 h APF window of IFM development requires a functionally and structurally sound NMJ for morphogenesis of the adult neuromuscular system. Furthermore, the immediate and latent effects of MeHg on expression of NMJ factors (*nlg/nrx*) correspond to impaired function of the neuromuscular system for flight. More broadly, our results highlight the dynamic and sensitive nature of the developing neuromuscular system and demonstrate that altering a single structural-based factor, such as Nlg1, can have persistent effects on neuromuscular function in the adult.

MeHg-mediated alteration of Nlg1 abundance could be influencing neuromuscular and NMJ morphology in several ways. First, we observed a decrease in the extent of DLM innervation by the ISN motor neuron in 7d adults with developmental MeHg exposure and this correlated with a decrease in flight ability. During metamorphosis, presynaptic Nrx1 and postsynaptic Nlg1 create adhesion complexes that are required for the "stick-and-grow" mechanism of axonal arborization in developing abdominal muscles. Interestingly, these complexes facilitate stable muscle-neuron attachments without the need of neurotransmitter release machinery or functional synapses (Constance *et al.*, 2018). Of note, IFM innervation is actively established during the first 24 h of metamorphosis, such that extensive branching and arborization is occurring at 14–18 h APF and the initial innervation pattern is established at 24 h APF (Fernandes and Vijayraghavan, 1993). Blocking neurotransmission between 12–20 and 20–26 h APF did not impact IFM morphology or adult flight ability, indicating that functional synapses are not required during this time. However, Nlg1 in muscle, acting nonautonomously, could be required for establishment of the ISN innervation pattern as studies have shown Nlg1 can influence axonal neurite arborization in adult

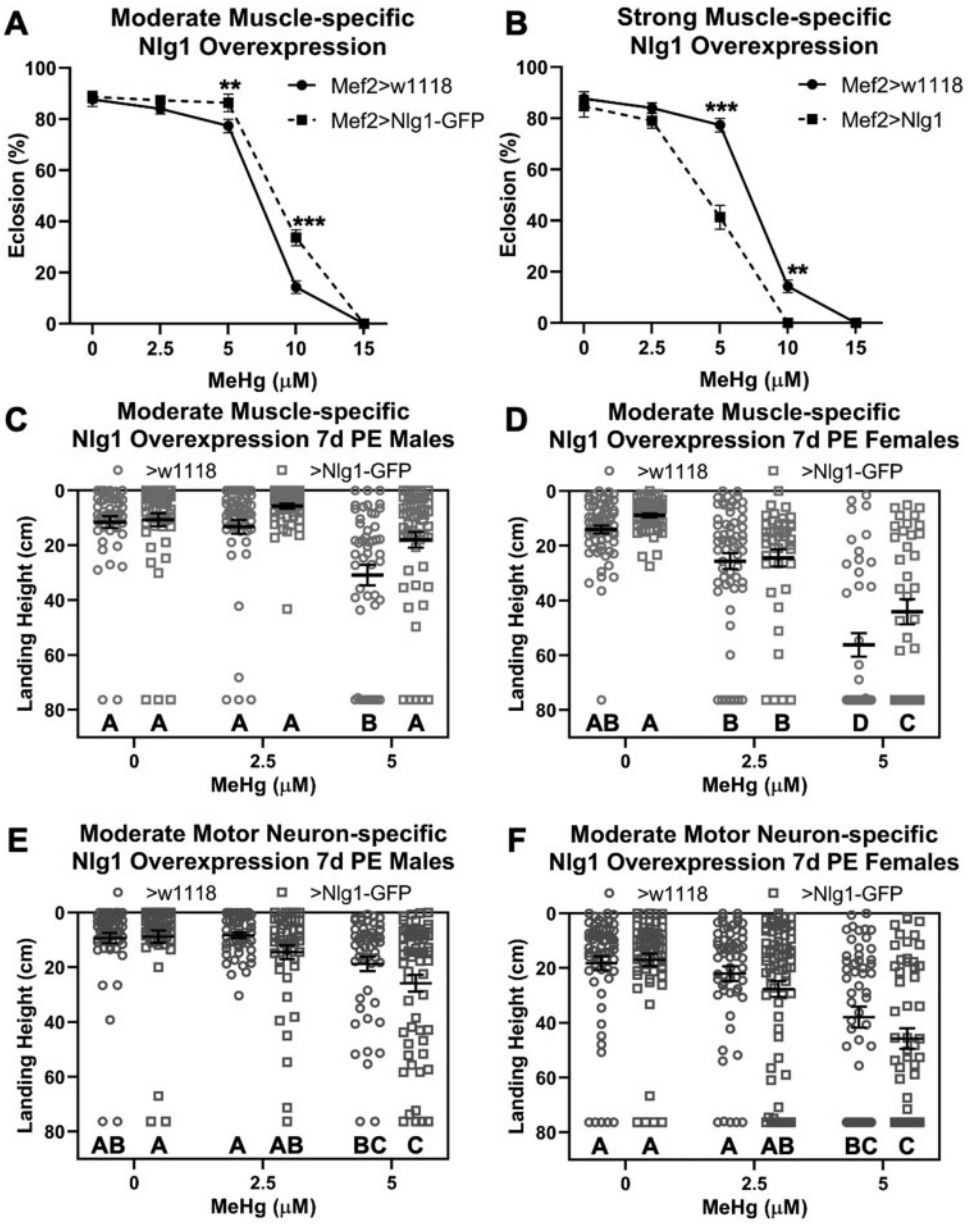

Figure 8. Moderate muscle-specific *nlg1* overexpression rescues neuromotor functions from MeHg. The impact of (A) moderate (>Nlg1-GFP) or (B) strong (>Nlg1) muscle-specific overexpression on eclosion compared with control (>w1118) upon developmental MeHg exposure ($n = 3$, 450 flies/genotype/treatment, mean ± SEM, *z* test, $^{**}p < .01$, $^{***}p < .001$). Landing height of 7d PE (C, E) males or (D, F) females with moderate muscle-specific (C, D) or motor neuron-specific (E, F) *nlg1* overexpression compared with control with developmental MeHg exposure ($n \geq 38$ individuals/genotype/treatment/sex, mean ± SEM, $p < .05$, 2-way ANOVA with Tukey's post hoc within each sex, significant differences indicated by different letter labels).

abdominal neurons (Constance *et al.*, 2018). Thus, when developmental MeHg exposure reduces *nlg1* expression between 20 and 36 h APF, the muscle-neuron interactions mediated by Nrx1-Nlg1 adhesion complexes could be insufficient to support the arborization, leading to less extensive branching.

Second, through decreasing Nlg1 abundance at the NMJ, MeHg may inhibit NMJ maturation during IFM development leading to poorer neuromuscular function. NMJ maturation begins at 24 h APF and continues throughout metamorphosis. MeHg repressed *nlg1* expression from 20–36 h APF, which may hinder initial NMJ maturation. Nlg1 has been shown to regulate NMJ bouton number, glutamate receptor recruitment, F-actin assembly, and presynaptic localization of Nrx1, such that these perturbation in structural components of the NMJ lead to decrease synaptic activity (Banerjee *et al.*, 2017; Banovic *et al.*, 2010; Owald *et al.*, 2012; Xing *et al.*, 2018). Although proving technically difficult here, future attempts at imaging IFM NMJs after developmental MeHg exposure will illuminate the Nlg1 sensitivity of NMJ maturation.

Despite evidence implicating Nlg1 as a mediator of MeHg neuromuscular toxicity, there are several limitations to consider. First, the doses employed for this study are higher than would be considered relevant human exposures (Diez, 2009). Nonetheless, it is typical that studies in laboratory animal models, both vertebrate and invertebrate, use MeHg doses in excess of that seen with human exposures in order to elaborate relevant toxicity mechanism and pathways (Castoldi *et al.*, 2008; Rand *et al.*, 2019; Schetinger *et al.*, 2019). As a point of reference,

flight deficits were seen after rearing flies on 2.5–5 μM MeHg food, which is equivalent to 0.5–1 ppm, and typically yields approximately 10–20 ppm Hg body burden. Hg amounts of 0.2–2.0 ppm are commonly seen tuna and swordfish consumed by humans. Cases of pathological MeHg poisoning in humans diagnosed with Minamata disease reported brain MeHg concentrations ranging between 2.6 and 24.8 ppm MeHg (Harada, 1995). Second, the MeHg effects were not evaluated at the level of protein expression for these NMJ factors, largely due to the unavailability of appropriate antibodies. Nonetheless, relating RNA transcript levels to functional endpoints of development or behavior, particularly where controlled and targeted manipulations (eg, GAL4 > UAS) are utilized, has conventionally been accepted as strong evidence for supporting hypotheses. Third, genetic manipulations of *Keap1 and nlg1* may have off target effects on other Drosophila behaviors which may confound our interpretation of flight and eclosion behavior. Although it is difficult to account for all behaviors, the *Keap1 and nlg1* manipulations broadly showed no effect on flight and eclosion and only appeared to influence the MeHg toxicity upon these behaviors.

Translating our findings to a mammalian model will be an important step in understanding Nlg and Nrx as players in MeHg neuromuscular toxicity. Humans and Drosophila contain 5 and 4 neuroligin genes, respectively, all of which share significant amino acid sequence similarity and evolved from a common ancestor (Banovic *et al.*, 2010; Chen *et al.*, 2012; Knight *et al.*, 2011; Sun and Xie, 2012). Thus, another limitation of this study is that the direct vertebrate homolog of Drosophila Nlg1 remains to be assigned (Sun *et al.*, 2011). However, in both Drosophila and humans, each neuroligin gene has a unique tissue expression pattern providing evidence for differential functions or roles in various neuromuscular compartments. Human neuroligin 1 (NLGN1) and neuroligin 2 (NLGN2) are the only brain-specific forms, with specificity to excitatory and inhibitory neurons, respectively (Chubykin *et al.*, 2007; Song *et al.*, 1999). Both human neuroligin 3 and 4X (NLGN3, NLGN4X) are expressed widely in peripheral tissues, including heart, liver, skeletal muscle, and pancreas (Lise and El-Husseini, 2006). Whereas NLGN3 is also found in the brain, NLGN4X is not (Bolliger *et al.*, 2001). Much research has focused on the roles of single-nucleotide polymorphisms and mutations in NLGNs as risk factors for neurodevelopmental disorders, especially autism (Bang and Owczarek, 2013; Lise and El-Husseini, 2006; Nakanishi *et al.*, 2017; Rothwell *et al.*, 2014). Less is known about their roles in peripheral tissues, but recent evidence indicates that NLGN3 and 4X and Nuerexin1 assist in controlling smooth muscle contractions of the gut (Hosie *et al.*, 2019; Li *et al.*, 2018). The fact that NLGN3 and NLGN4X are expressed in skeletal muscle and have been implicated in regulating smooth muscle contractions supports the continued investigation of transsynaptic communication between neuroligins and neurexins at the vertebrate skeletal muscle NMJ upon MeHg exposure.

Consistent with our prior report (Gunderson *et al.*, 2020), we show that MeHg toxicity can be moderated through induction of the Nrf2. The Nrf2 pathway is well described for its protective effects toward MeHg-induced oxidative stress (Ni *et al.*, 2010; Toyama *et al.*, 2007; Wang *et al.*, 2009). However, across several animal models, including *C. elegans*, Drosophila, and rodents, the Nrf2 transcription factor is known to regulate genes involved in a variety of cellular processes outside the conventional antioxidant response (He *et al.*, 2020; Pitoniak and Bohmann, 2015), which in turn respond differently under various stress, developmental, or aging paradigms (Deng and Kerppola, 2013; Lacher *et al.*, 2015; TonelLi *et al.*, 2018; Tsakiri *et al.*, 2019). Of note, in *C. elegans*, the Nrf2 homolog, skn-1, regulates neuroligin expression, with increased neuroligin at the NMJ protecting against toxicant-induced oxidative stress (Staab *et al.*, 2014). We propose a possible role of Drosophila Nrf2 regulating *nlg1* expression in developing muscle to facilitate the proper maturation of NMJs. Drosophila Nrf2 signaling is known to regulate fundamental developmental processes under homeostatic conditions (Deng and Kerppola, 2013). With developmental MeHg exposure, where Nrf2 signaling is induced (Gunderson *et al.*, 2020), we surmise that the Nrf2 transcription factor is sequestered to upregulate antioxidant response genes, which may diminish its occupancy on developmental genes. Within a given cellular context, Nrf2 has been shown to shift to preferentially induce the expression of certain types or batteries of genes (Tsakiri *et al.*, 2019). Here, we hypothesize that the observed increase in antioxidant gene expression (Gunderson *et al.*, 2020) and a simultaneous down regulation in *nlg1* expression at 24 h APF due to development exposure to 10 μM MeHg may result from a shift in Nrf2 occupancy away from fundamental development genes targets, which may include *nlg1*. In support of this, muscle-specific *Keap1* knockdown (Mef2 > Keap1^{RNAi}), which transgenically activates Nrf2 signaling, increases the expression of *nlg1*, *nlg2*, and *nlg3*, but not *nrx1* at 24 h APF (Gunderson and Rand, unpublished observations). Thus, one mechanism by which flight is rescued through muscle-specific *Keap1* knockdown is through partial rescue in *nlg1* expression. The relationship of Nrf2 and Nlg1 will require additional investigation.

SUPPLEMENTARY DATA

Supplementary data are available at *Toxicological Sciences* online.

ACKNOWLEDGMENTS

We thank University of Rochester Drosophila researchers for communal fly husbandry materials and helpful discussions during meetings, including D. Cory-Slechta, D. Bohmann, and D. Anderson. We thank all members of the Rand laboratory for the critical feedback during the course of the study. We are especially grateful to D. Bohmann and R. Hoff (University of Rochester) and H. Aberle (Heinrich Heine University Düsseldorf) for providing many of the fly strains used in this study.

FUNDING

National Institute of Environmental Health Sciences (R01 ES025721 [PI; M.D.R.], R01 ES010219 [co-I; M.D.R.], P30 ES001247 [co-I; M.D.R.]); the University of Rochester Environmental Health Sciences Center (T32 207026 to J.G.).

DECLARATION OF CONFLICTING INTERESTS

The authors declared no potential conflicts of interest with respect to the research, authorship, and/or publication of this article.

REFERENCES

Antunes Dos Santos, A., Appel Hort, M., Culbreth, M., Lopez-Granero, C., Farina, M., Rocha, J. B., and Aschner, M. (2016). Methylmercury and brain development: A review of recent literature. *J. Trace Elem. Med. Biol.* **38**, 99–107.

Atchison, W. D., and Narahashi, T. (1982). Methylmercury-induced depression of neuromuscular transmission in the rat. *Neurotoxicology* **3**, 37–50.

Bakir, F., Damluji, S. F., Amin-Zaki, L., Murtadha, M., Khalidi, A., al-Rawi, N. Y., Tikriti, S., Dahahir, H. I., Clarkson, T. W., Smith, J. C., *et al.* (1973). Methylmercury poisoning in Iraq. *Science* **181**, 230–241.

Banerjee, S., Venkatesan, A., and Bhat, M. A. (2017). Neurexin, neuroligin and wishful thinking coordinate synaptic cytoarchitecture and growth at neuromuscular junctions. *Mol. Cell. Neurosci.* **78**, 9–24.

Bang, M. L., and Owczarek, S. (2013). A matter of balance: Role of neurexin and neuroligin at the synapse. *Neurochem. Res.* **38**, 1174–1189.

Banovic, D., Khorramshahi, O., Owald, D., Wichmann, C., Riedt, T., Fouquet, W., Tian, R., Sigrist, S. J., and Aberle, H. (2010). Drosophila neuroligin 1 promotes growth and postsynaptic differentiation at glutamatergic neuromuscular junctions. *Neuron* **66**, 724–738.

Bolliger, M. F., Frei, K., Winterhalter, K. H., and Gloor, S. M. (2001). Identification of a novel neuroligin in humans which binds to PSD-95 and has a widespread expression. *Biochem. J.* **356**, 581–588.

Brand, A. H., and Perrimon, N. (1993). Targeted gene expression as a means of altering cell fates and generating dominant phenotypes. *Development* **118**, 401–415.

Burke, K., Cheng, Y., Li, B., Petrov, A., Joshi, P., Berman, R. F., Reuhl, K. R., and DiCicco-Bloom, E. (2006). Methylmercury elicits rapid inhibition of cell proliferation in the developing brain and decreases cell cycle regulator, cyclin E. *Neurotoxicology* **27**, 970–981.

Candura, S. M., D'Agostino, G., Castoldi, A. F., Messori, E., Liuzzi, M., Manzo, L., and Tonini, M. (1997). Effects of mercuric chloride and methyl mercury on cholinergic neuromuscular transmission in the guinea-pig ileum. *Pharmacol. Toxicol.* **80**, 218–224.

Carratu, M. R., Borracci, P., Coluccia, A., Giustino, A., Renna, G., Tomasini, M. C., Raisi, E., Antonelli, T., Cuomo, V., Mazzoni, E., *et al.* (2006). Acute exposure to methylmercury at two developmental windows: Focus on neurobehavioral and neurochemical effects in rat offspring. *Neuroscience* **141**, 1619–1629.

Castoldi, A. F., Onishchenko, N., Johansson, C., Coccini, T., Roda, E., Vahter, M., Ceccatelli, S., and Manzo, L. (2008). Neurodevelopmental toxicity of methylmercury: Laboratory animal data and their contribution to human risk assessment. *Regul. Toxicol. Pharmacol.* **51**, 215–229.

Chen, C., Amirbahman, A., Fisher, N., Harding, G., Lamborg, C., Nacci, D., and Taylor, D. (2008). Methylmercury in marine ecosystems: Spatial patterns and processes of production, bioaccumulation, and biomagnification. *Ecohealth* **5**, 399–408.

Chen, M. S., Burgess, C. C., Vallee, R. B., and Wadsworth, S. C. (1992). Developmental stage- and tissue-specific expression of shibire, a Drosophila gene involved in endocytosis. *J. Cell Sci.* **103**(Pt 3), 619–628.

Chen, M. S., Obar, R. A., Schroeder, C. C., Austin, T. W., Poodry, C. A., Wadsworth, S. C., and Vallee, R. B. (1991). Multiple forms of dynamin are encoded by shibire, a Drosophila gene involved in endocytosis. *Nature* **351**, 583–586.

Chen, Y. C., Lin, Y. Q., Banerjee, S., Venken, K., Li, J., Ismat, A., Chen, K., Duraine, L., Bellen, H. J., and Bhat, M. A. (2012). Drosophila neuroligin 2 is required presynaptically and postsynaptically for proper synaptic differentiation and synaptic transmission. *J. Neurosci.* **32**, 16018–16030.

Chubykin, A. A., Atasoy, D., Etherton, M. R., Brose, N., Kavalali, E. T., Gibson, J. R., and Sudhof, T. C. (2007). Activity-dependent validation of excitatory versus inhibitory synapses by neuroligin-1 versus neuroligin-2. *Neuron* **54**, 919–931.

Constance, W. D., Mukherjee, A., Fisher, Y. E., Pop, S., Blanc, E., Toyama, Y., and Williams, D. W. (2018). Neurexin and Neuroligin-based adhesion complexes drive axonal arborisation growth independent of synaptic activity. *Elife* **7**, 1–33.

Culbreth, M., and Rand, M. D. (2020). Methylmercury modifies temporally expressed myogenic regulatory factors to inhibit myoblast differentiation. *Toxicol. In Vitro* **63**, 104717.

Cunningham, P., Cooter, W., and Sullivan, E. (2003). Mercury in Marine Life Database. In *Mercury in Marine Life Database* (U.S.E.P. Agency, Ed.), pp. 1–226. U.S. EPA, Washington, DC.

Daniels, R. W., Gelfand, M. V., Collins, C. A., and DiAntonio, A. (2008). Visualizing glutamatergic cell bodies and synapses in Drosophila larval and adult CNS. *J. Comp. Neurol.* **508**, 131–152.

Deng, H., and Kerppola, T. K. (2013). Regulation of Drosophila metamorphosis by xenobiotic response regulators. *PLoS Genet.* **9**, e1003263.

Diez, S. (2009). Human health effects of methylmercury exposure. *Rev. Environ. Contam. Toxicol.* **198**, 111–132.

Ekino, S., Susa, M., Ninomiya, T., Imamura, K., and Kitamura, T. (2007). Minamata disease revisited: An update on the acute and chronic manifestations of methyl mercury poisoning. *J. Neurol. Sci.* **262**, 131–144.

Engel, G. L., and Rand, M. D. (2014). The Notch target E(spl)mdelta is a muscle-specific gene involved in methylmercury toxicity in motor neuron development. *Neurotoxicol. Teratol.* **43**, 11–18.

Fernandes, J., Bate, M., and Vijayraghavan, K. (1991). Development of the indirect flight muscles of Drosophila. *Development* **113**, 67–77.

Fernandes, J., and Vijayraghavan, K. (1993). The development of indirect flight muscle innervation in Drosophila melanogaster. *Development* **118**, 215–227.

Fernandes, J. J., and Keshishian, H. (1998). Nerve-muscle interactions during flight muscle development in Drosophila. *Development* **125**, 1769–1779.

Fujimura, M., Cheng, J., and Zhao, W. (2012). Perinatal exposure to low-dose methylmercury induces dysfunction of motor coordination with decreases in synaptophysin expression in the cerebellar granule cells of rats. *Brain Res.* **1464**, 1–7.

Fujimura, M., and Usuki, F. (2015). Methylmercury causes neuronal cell death through the suppression of the TrkA pathway: In vitro and in vivo effects of TrkA pathway activators. *Toxicol. Appl. Pharmacol.* **282**, 259–266.

Fujimura, M., Usuki, F., Cheng, J., and Zhao, W. (2016). Prenatal low-dose methylmercury exposure impairs neurite outgrowth and synaptic protein expression and suppresses TrkA pathway activity and eEF1A1 expression in the rat cerebellum. *Toxicol. Appl. Pharmacol.* **298**, 1–8.

Fujimura, M., Usuki, F., Sawada, M., Rostene, W., Godefroy, D., and Takashima, A. (2009). Methylmercury exposure downregulates the expression of Racl and leads to neuritic degeneration and ultimately apoptosis in cerebrocortical neurons. *Neurotoxicology* **30**, 16–22.

Gonzalez, P., Dominique, Y., Massabuau, J. C., Boudou, A., and Bourdineaud, J. P. (2005). Comparative effects of dietary methylmercury on gene expression in liver, skeletal muscle, and brain of the zebrafish (Danio rerio). *Environ. Sci. Technol.* **39**, 3972–3980.

Groth, E. 3rd (2010). Ranking the contributions of commercial fish and shellfish varieties to mercury exposure in the United

States: Implications for risk communication. *Environ. Res.* **110**, 226–236.

Gunderson, J. T., Peppriell, A. E., Vorojeikina, D., and Rand, M. D. (2020). Tissue-specific Nrf2 signaling protects against methylmercury toxicity in Drosophila neuromuscular development. *Arch. Toxicol.* **94**, 4007–4022.

Harada, M. (1995). Minamata disease: Methylmercury poisoning in Japan caused by environmental pollution. *Crit. Rev. Toxicol.* **25**, 1–24.

He, F., Ru, X., and Wen, T. (2020). NRF2, a Transcription Factor for Stress Response and Beyond. *Int. J. Mol. Sci.* **21**, 1–23.

Hebbar, S., and Fernandes, J. J. (2004). Pruning of motor neuron branches establishes the DLM innervation pattern in Drosophila. *J. Neurobiol.* **60**, 499–516.

Hong, Y. S., Kim, Y. M., and Lee, K. E. (2012). Methylmercury exposure and health effects. *J. Prev. Med. Public Health* **45**, 353–363.

Hosie, S., Ellis, M., Swaminathan, M., Ramalhosa, F., Seger, G. O., Balasuriya, G. K., Gillberg, C., Rastam, M., Churilov, L., McKeown, S. J., *et al.* (2019). Gastrointestinal dysfunction in patients and mice expressing the autism-associated R451C mutation in neuroligin-3. *Autism Res.* **12**, 1043–1056.

Hummon, M. R., and Costello, W. J. (1988). Induced neuroma formation and target muscle perturbation in the giant fiber pathway of the Drosophila temperature-sensitive mutant shibire. *Rouxs Arch. Dev. Biol.* **197**, 383–393.

Hummon, M. R., and Costello, W. J. (1993). Flight muscle formation inDrosophila mosaics: Requirement for normalshibire function of endocytosis. *Rouxs Arch. Dev. Biol.* **202**, 95–102.

Hunter, J. W., Mullen, G. P., McManus, J. R., Heatherly, J. M., Duke, A., and Rand, J. B. (2010). Neuroligin-deficient mutants of *C. elegans* have sensory processing deficits and are hypersensitive to oxidative stress and mercury toxicity. *Dis. Model. Mech.* **3**, 366–376.

Knight, D., Xie, W., and Boulianne, G. L. (2011). Neurexins and neuroligins: Recent insights from invertebrates. *Mol. Neurobiol.* **44**, 426–440.

Koenig, J. H., and Ikeda, K. (1983). Evidence for a presynaptic blockage of transmission in a temperature-sensitive mutant of Drosophila. *J. Neurobiol.* **14**, 411–419.

Koenig, J. H., and Ikeda, K. (1989). Disappearance and reformation of synaptic vesicle membrane upon transmitter release observed under reversible blockage of membrane retrieval. *J. Neurosci.* **9**, 3844–3860.

Koenig, J. H., Saito, K., and Ikeda, K. (1983). Reversible control of synaptic transmission in a single gene mutant of Drosophila melanogaster. *J. Cell Biol.* **96**, 1517–1522.

Lacher, S. E., Lee, J. S., Wang, X., Campbell, M. R., Bell, D. A., and Slattery, M. (2015). Beyond antioxidant genes in the ancient Nrf2 regulatory network. *Free Radic. Biol. Med.* **88**, 452–465.

Li, Y., Liu, H., and Dong, Y. (2018). Significance of neurexin and neuroligin polymorphisms in regulating risk of Hirschsprung's disease. *J. Investig. Med.* **66**, 1.3–8.

Lise, M. F., and El-Husseini, A. (2006). The neuroligin and neurexin families: From structure to function at the synapse. *Cell. Mol. Life Sci.* **63**, 1833–1849.

Livak, K. J., and Schmittgen, T. D. (2001). Analysis of relative gene expression data using real-time quantitative PCR and the 2(-delta delta C(t)) method. *Methods* **25**, 402–408.

Mahapatra, C. T., Bond, J., Rand, D. M., and Rand, M. D. (2010). Identification of methylmercury tolerance gene candidates in Drosophila. *Toxicol. Sci.* **116**, 225–238.

Mahr, A., and Aberle, H. (2006). The expression pattern of the Drosophila vesicular glutamate transporter: A marker protein for motoneurons and glutamatergic centers in the brain. *Gene Expr. Patterns* **6**, 299–309.

McKeown-Eyssen, G. E., Ruedy, J., and Neims, A. (1983). Methyl mercury exposure in northern Quebec. II. Neurologic findings in children. *Am. J. Epidemiol.* **118**, 470–479.

Mellingen, R. M., Myrmel, L. S., Lie, K. K., Rasinger, J. D., Madsen, L., and Nostbakken, O. J. (2021). RNA sequencing and proteomic profiling reveal different alterations by dietary methylmercury in the hippocampal transcriptome and proteome in BALB/c mice. *Metallomics* **13**, 1–12.

Montgomery, S. L., Vorojeikina, D., Huang, W., Mackay, T. F., Anholt, R. R., and Rand, M. D. (2014). Genome-wide association analysis of tolerance to methylmercury toxicity in Drosophila implicates myogenic and neuromuscular developmental pathways. *PLoS One* **9**, e110375.

Nakanishi, M., Nomura, J., Ji, X., Tamada, K., Arai, T., Takahashi, E., Bucan, M., and Takumi, T. (2017). Functional significance of rare neuroligin 1 variants found in autism. *PLoS Genet.* **13**, e1006940.

Ni, M., Li, X., Yin, Z., Jiang, H., Sidoryk-Wegrzynowicz, M., Milatovic, D., Cai, J., and Aschner, M. (2010). Methylmercury induces acute oxidative stress, altering Nrf2 protein level in primary microglial cells. *Toxicol. Sci.* **116**, 590–603.

Owald, D., Khorramshahi, O., Gupta, V. K., Banovic, D., Depner, H., Fouquet, W., Wichmann, C., Mertel, S., Eimer, S., Reynolds, E., *et al.* (2012). Cooperation of Syd-1 with Neurexin synchronizes pre- with postsynaptic assembly. *Nat. Neurosci.* **15**, 1219–1226.

Peppriell, A. E., Gunderson, J. T., Vorojeikina, D., and Rand, M. D. (2020). Methylmercury myotoxicity targets formation of the myotendinous junction. *Toxicology* **443**, 152561.

Pitoniak, A., and Bohmann, D. (2015). Mechanisms and functions of Nrf2 signaling in Drosophila. *Free Radic. Biol. Med.* **88**, 302–313.

Poulopoulos, A., Aramuni, G., Meyer, G., Soykan, T., Hoon, M., Papadopoulos, T., Zhang, M., Paarmann, I., Fuchs, C., Harvey, K., *et al.* (2009). Neuroligin 2 drives postsynaptic assembly at perisomatic inhibitory synapses through gephyrin and collybistin. *Neuron* **63**, 628–642.

Prince, L. M., and Rand, M. D. (2017). Notch target gene E(spl)mdelta is a mediator of methylmercury-induced myotoxicity in Drosophila. *Front. Genet.* **8**, 233.

Prince, L. M., and Rand, M. D. (2018). Methylmercury exposure causes a persistent inhibition of myogenin expression and C2C12 myoblast differentiation. *Toxicology* **393**, 113–122.

Rand, M. D., Dao, J. C., and Clason, T. A. (2009). Methylmercury disruption of embryonic neural development in Drosophila. *Neurotoxicology* **30**, 794–802.

Rand, M. D., Montgomery, S. L., Prince, L., and Vorojeikina, D. (2014). Developmental toxicity assays using the Drosophila model. *Curr. Protoc. Toxicol.* **59**, 1.12.1–20.

Rand, M. D., Vorojeikina, D., Pepriell, P., Gunderson, J., and Prince, L. (2019). Drosophotoxicology: Elucidating kinetic and dynamic pathways of methylmercury toxicity in a Drosophila model. *Front. Genet.* **10**, 1–16.

Rodier, P. M., Aschner, M., and Sager, P. R. (1984). Mitotic arrest in the developing CNS after prenatal exposure to methylmercury. *Neurobehav. Toxicol. Teratol.* **6**, 379–385.

Rothwell, P. E., Fuccillo, M. V., Maxeiner, S., Hayton, S. J., Gokce, O., Lim, B. K., Fowler, S. C., Malenka, R. C., and Sudhof, T. C. (2014). Autism-associated neuroligin-3 mutations commonly impair striatal circuits to boost repetitive behaviors. *Cell* **158**, 198–212.

Sager, P. R., Aschner, M., and Rodier, P. M. (1984). Persistent, differential alterations in developing cerebellar cortex of male

and female mice after methylmercury exposure. *Brain Res.* **314**, 1–11.

Schetinger, M. R. C., Peres, T. V., Arantes, L. P., Carvalho, F., Dressler, V., Heidrich, G., Bowman, A. B., and Aschner, M. (2019). Combined exposure to methylmercury and manganese during L1 larval stage causes motor dysfunction, cholinergic and monoaminergic up-regulation and oxidative stress in L4 *Caenorhabditis elegans*. *Toxicology* **411**, 154–162.

Schulman, V. K., Dobi, K. C., and Baylies, M. K. (2015). Morphogenesis of the somatic musculature in *Drosophila melanogaster*. *Wiley Interdiscip. Rev. Dev. Biol.* **4**, 313–334.

Sink, H. (2006). *Muscle Development in Drosophila*. Molecular Biology Intelligence Unit. Springer, New York, NY. doi: 10.1007/0-387-32963-3. Accessed May 13, 2021.

Song, J. Y., Ichtchenko, K., Sudhof, T. C., and Brose, N. (1999). Neuroligin 1 is a postsynaptic cell-adhesion molecule of excitatory synapses. *Proc. Natl. Acad. Sci. U.S.A.* **96**, 1100–1105.

Spletter, M. L., Barz, C., Yeroslaviz, A., Zhang, X., Lemke, S. B., Bonnard, A., Brunner, E., Cardone, G., Basler, K., Habermann, B. H., *et al.* (2018). A transcriptomics resource reveals a transcriptional transition during ordered sarcomere morphogenesis in flight muscle. *Elife* **7**, 1–132.

Staab, T. A., Evgrafov, O., Egrafov, O., Knowles, J. A., and Sieburth, D. (2014). Regulation of synaptic nlg-1/neuroligin abundance by the skn-1/Nrf stress response pathway protects against oxidative stress. *PLoS Genet.* **10**, e1004100.

Sun, M., and Xie, W. (2012). Cell adhesion molecules in Drosophila synapse development and function. *Sci. China Life Sci.* **55**, 20–26.

Sun, M., Xing, G., Yuan, L., Gan, G., Knight, D., With, S. I., He, C., Han, J., Zeng, X., Fang, M., *et al.* (2011). Neuroligin 2 is required for synapse development and function at the Drosophila neuromuscular junction. *J. Neurosci.* **31**, 687–699.

Swank, D. M. (2012). Mechanical analysis of Drosophila indirect flight and jump muscles. *Methods* **56**, 69–77.

Tabuchi, K., and Sudhof, T. C. (2002). Structure and evolution of neurexin genes: Insight into the mechanism of alternative splicing. *Genomics* **79**, 849–859.

Teng, X., Zhang, Z., He, G., Yang, L., and Li, F. (2012). Validation of reference genes for quantitative expression analysis by real-time RT-PCR in four lepidopteran insects. *J. Insect Sci.* **12**, 60.

Tonelli, C., Chio, I. I. C., and Tuveson, D. A. (2018). Transcriptional regulation by Nrf2. *Antioxid. Redox Signal.* **29**, 1727–1745.

Toyama, T., Sumi, D., Shinkai, Y., Yasutake, A., Taguchi, K., Tong, K. I., Yamamoto, M., and Kumagai, Y. (2007). Cytoprotective role of Nrf2/Keap1 system in methylmercury toxicity. *Biochem. Biophys. Res. Commun.* **363**, 645–650.

Tsakiri, E. N., Gumeni, S., Iliaki, K. K., Benaki, D., Vougas, K., Sykiotis, G. P., Gorgoulis, V. G., Mikros, E., Scorrano, L., and Trougakos, I. P. (2019). Hyperactivation of Nrf2 increases stress tolerance at the cost of aging acceleration due to metabolic deregulation. *Aging Cell* **18**, e12845.

Usuki, F., Yasutake, A., Matsumoto, M., and Higuchi, I. (2001). Chronic low-dose Methylmercury administration decreases mitochondrial enzyme activities and induces myopathic changes in rats. *J. Health Sci.* **47**, 162–167.

Usuki, F., Yasutake, A., Matsumoto, M., Umehara, F., and Higuchi, I. (1998). The effect of methylmercury on skeletal muscle in the rat: A histopathological study. *Toxicol. Lett.* **94**, 227–232.

Varoqueaux, F., Aramuni, G., Rawson, R. L., Mohrmann, R., Missler, M., Gottmann, K., Zhang, W., Sudhof, T. C., and Brose, N. (2006). Neuroligins determine synapse maturation and function. *Neuron* **51**, 741–754.

Wang, L., Jiang, H., Yin, Z., Aschner, M., and Cai, J. (2009). Methylmercury toxicity and Nrf2-dependent detoxification in astrocytes. *Toxicol. Sci.* **107**, 135–143.

Xing, G., Gan, G., Chen, D., Sun, M., Yi, J., Lv, H., Han, J., and Xie, W. (2014). Drosophila neuroligin3 regulates neuromuscular junction development and synaptic differentiation. *J. Biol. Chem.* **289**, 31867–31877.

Xing, G., Li, M., Sun, Y., Rui, M., Zhuang, Y., Lv, H., Han, J., Jia, Z., and Xie, W. (2018). Neurexin-neuroligin 1 regulates synaptic morphology and functions via the WAVE regulatory complex in Drosophila neuromuscular junction. *Elife* **7**, 1–23.

Zhang, X., Rui, M., Gan, G., Huang, C., Yi, J., Lv, H., and Xie, W. (2017). Neuroligin 4 regulates synaptic growth via the bone morphogenetic protein (BMP) signaling pathway at the Drosophila neuromuscular junction. *J. Biol. Chem.* **292**, 17991–18005.